Supplemental Material

Article Title:

Disposition and Metabolism of [^{14}C]Lemborexant in Healthy Human Subjects and Characterization of Its Circulating Metabolites

Authors:

Takashi Ueno, Tomomi Ishida, Jagadeesh Aluri, Michiyuki Suzuki, Carsten T. Beuckmann, Takaaki Kameyama, Shoji Asakura, Kazutomi Kusano

Journal Title:

Drug Metabolism and Disposition

Manuscript Number:

DMD-AR-2020-000229

Supplemental Data

Rationale for structural characterization of metabolites.

M3, M4, M9, and M10: Each metabolite showed a molecular ion $[M+H]^+$ at *m*/*z* 427, 16 Da higher than that of the parent, and fragment ions at *m*/*z* 287, 269, 175, 147, 141, 139, and 113. The fragment ion at *m*/*z* 141 suggests that lemborexant underwent mono-oxidation at the dimethylpyrimidine moiety. Based on the retention times of authentic standards, structures of M3 and M9 were identified as hydroxylated forms and those of M4 and M10 were identified as *N*-oxide metabolites.

M1 and M7: Both showed the molecular ion $[M+H]^+$ at *m*/*z* 427, 16 Da higher than that of the parent, and fragment ions at *m*/*z* 303, 285, 191, 163, 139, 125, and 113. The fragment ions at *m*/*z* 125 and 113 suggest that lemborexant underwent mono-oxidation at the fluorophenyl moiety. Based on the retention times of authentic standards, the structures of M1 and M7 were identified as hydroxylated forms of lemborexant.

M8: M8 showed a molecular ion $[M+H]^+$ at *m*/*z* 427 and fragment ions at *m*/*z* 303, 285, 283, 175, 155, 147, 129, and 125. The fragment ion at *m*/*z* 129 suggests that lemborexant underwent mono-oxidation at the fluoropyridine moiety. Based on the retention time of an authentic standard, the structure of M8 was identified as a hydroxylated form with a rearrangement of the fluorine on the fluoropyridine moiety, attributed to a mechanism analogous to an NIH-shift.

M13, M14, and M15: Each metabolite showed a molecular ion $[M+H]^+$ at *m*/*z* 443, 32 Da higher than that of the parent, and fragment ions at *m*/*z* 287, 269, 175, 147, 139, and 113. M13 also showed a fragment ion at *m*/*z* 425, and M14 and M15 showed that at *m*/*z* 157. The fragment ion at *m*/*z* 287 suggests that di-oxidation occurred at the dimethylpyrimidine moiety. Comparing with fragment ions and retention times of authentic standards, M13, M14, and M15 were identified as di-oxidized metabolites.

Met15-1, Met15-2, and Met22-2: Each metabolite showed a molecular ion $[M+H]^+$ at *m*/*z* 443, 32 Da higher than that of the parent. Met15-1 and Met22-2 showed key fragment ions at *m*/*z* 319 and

207, suggesting that di-oxidation occurred at the fluoropyridine moiety. Met15-2 showed key fragment ions at 303 and 191, suggesting that mono-oxidation occurred at both dimethylpyrimidine and fluorophenyl moieties. Therefore, Met15-1, Met15-2, and Met22-2 were proposed to be di-oxidized metabolites.

M16, M17, M18, M20, and M21: Each metabolite showed a molecular ion $[M+H]^+$ at *m*/*z* 603, 192 Da higher than that of the parent. Their fragment ions and retention times were consistent with those of glucuronide conjugates, which were enzymatically generated from hydroxylated metabolites, M1, M5, M3, M8, and M9, respectively, in human liver microsomes fortified with uridine 5′-diphospho-glucuronic acid (UDPGA). Therefore, M16, M17, M18, M20, and M21 were identified as glucuronide conjugates of M1, M5, M3, M8, and M9, respectively.

M23, M24, Met9-2, Met9-3, Met11-2, and Met11-3: Each metabolite showed a molecular ion $[M+H]^+$ at *m*/*z* 619, 208 Da higher than that of the parent, suggesting that these metabolites were glucuronide conjugates of di-oxidized metabolites. M23, M24, and Met9-3 showed a key fragment ion at *m*/*z* 287, suggesting that di-oxidation and glucuronidation occurred at the dimethylpyrimidine moiety. The fragment ions and retention times of M23 and M24 were consistent with those of glucuronide conjugates that were enzymatically generated from M13 and M14 in human liver microsomes fortified with UDPGA. Thus, the structures of M23 and M24 were identified as glucuronide conjugates of M13 and M14, respectively. Met11-2 showed key fragment ions at *m*/*z* 495 and 207, suggesting that di-oxidation and glucuronidation occurred at the fluorophenyl moiety. The structures of Met9-2 and Met11-3 could not be further characterized based on the fragmentation patterns.

Met14-1 and Met19: Each metabolite showed a molecular ion $[M+H]^+$ at *m*/*z* 507, 96 Da higher than that of the parent, suggesting that these metabolites were sulfate conjugates of mono-oxidized metabolites. Met14-1 and M19 showed key fragment ions at *m*/*z* 191 and 287, respectively, suggesting that mono-oxidation and sulfation occurred at the fluorophenyl and dimethylpyrimidine moieties, respectively.

M11: M11 showed a molecular ion $[M+H]^+$ at *m*/*z* 317, 94 Da lower than that of the parent, and fragment ions at *m*/*z* 193 and 125. Comparing with fragment ions and retention time of an authentic standard, M11 was identified as a hydrolyzed form of lemborexant.

M22: M22 showed a molecular ion $[M+H]^+$ at *m*/*z* 493, 82 Da lower than that of the parent, and fragment ions at *m*/*z* 317, 193, and 125. The fragment ions and retention time of M11 were consistent with those of a glucuronide conjugate that was enzymatically generated from M11 in human liver microsomes fortified with UDPGA. Thus, the structure of M11 was identified as a glucuronide conjugate of M11.

Met16-1: Met16-1 showed a molecular ion $[M+H]^+$ at *m*/*z* 333, 78 Da lower than that of the parent. Key fragment ions at *m*/*z* 193 and 141 suggest that amide hydrolysis and mono-oxidation occurred at the dimethylprimidine moiety. Therefore, Met16-1 was proposed to be a mono-oxidized metabolite of M11.

Met5: Met5 showed a molecular ion $[M+H]^+$ at *m*/*z* 445, 34 Da higher than that of the parent. Key fragment ions at *m*/*z* 321, 191, and 113 suggest that lemborexant underwent di-oxidation and subsequent reduction at the fluorophenyl moiety. Thus, Met5 was proposed to be a dihydrodiol form of lemborexant.

M12: M12 showed a molecular ion $[M+H]^+$ at *m*/*z* 441, 30 Da higher than that of the parent, and fragment ions at *m*/*z* 287, 269, 175, 147, 139, and 113. The fragment ion at *m*/*z* 287 suggested that lemborexant underwent carboxylation at the dimethylprimidine moiety. Comparing with fragment ions and retention time of an authentic standard, M12 was identified as a carboxylated form of lemborexant.

Met14-2: Met14-2 showed a molecular ion $[M+H]^+$ at *m*/*z* 457, 46 Da higher than that of the parent. Key fragment ions at *m*/*z* 303 and 191 suggest that fluorophenyl moiety was oxidized and that dimethylpyrimidine moiety was carboxylated. Thus, Met14-2 was proposed to be a carboxylated form of a mono-oxidized metabolite.

Met29: Met29 showed a molecular ion $[M+H]^+$ at *m*/*z* 455, 44 Da higher than that of the parent. A key fragment ion at *m*/*z* 169 suggests that dimethylpyrimidine moiety was carboxylated and subsequently methylated. Thus, Met29 was proposed to be a methylated form of a carboxylated lemborexant.

Supplemental Table

Supplemental Table 1. Molecular ions and characteristic fragment ions of lemborexant and metabolites detected in biological samples.

ID	M-No.	Detection	Molecular formula	$[M+H]^+$		Δ ppm	Key fragment ions (*m*/*z*)
				Theoretical	Observed		
Parent	Lemborexant	P, F	$C_{22}H_{21}F_2N_4O_2$	411.16271	411.16318	1.1	287, 269, 175, 147, 139, 125, 113
Met1	—	P	Unknown	—	—	—	—
Met2	—	P	Unknown	—	—	—	—
Met3	—	P	Unknown	—	—	—	—
Met4	—	U	Unknown	—	—	—	—
Met5	—	P, U	$C_{22}H_{23}F_2N_4O_4$	445.16819	445.16757	–1.4	321, 303, 285, 191, 163, 139, 113
Met6	M23 (M13-Gluc)	U	$C_{28}H_{29}F_2N_4O_{10}$	619.18463	619.18472	0.1	443, 425, 287, 269, 175
Met7	—	P, U	Unknown	—	—	—	—
Met8	—	P	Unknown	—	—	—	—
Met9-1	M16 (M1-Gluc)	U	$C_{28}H_{29}F_2N_4O_9$	603.18971	603.18928	–0.7	479, 427, 303, 285, 191, 179, 163, 139, 125, 113
Met9-2	—	U	$C_{28}H_{29}F_2N_4O_{10}$	619.18463	619.18581	1.9	479, 443, 303, 285, 175, 155, 147, 141, 129
Met9-3	—	U	$C_{28}H_{29}F_2N_4O_{10}$	619.18463	619.18581	1.9	443, 287, 269, 175, 157, 147, 139, 113
Met9-4	M22 (M11-Gluc)	U	$C_{23}H_{26}FN_2O_9$	493.16169	493.15977	–3.9	317, 193, 125
Met10	—	F	Unknown	—	—	—	—
Met11-1	M17 (M5-Gluc)	U	$C_{28}H_{29}F_2N_4O_9$	603.18971	603.18958	–0.2	479, 427, 303, 285, 175, 155, 147, 129, 125
Met11-2	—	P, U	$C_{28}H_{29}F_2N_4O_{10}$	619.18463	619.18529	1.1	495, 443, 319, 301, 207, 179, 139, 113

Met11-3	—	U	$C_{28}H_{29}F_2N_4O_{10}$	619.18463	619.18603	2.3	443, 303
Met12	M18 (M3-Gluc)	P, U	$C_{28}H_{29}F_2N_4O_9$	603.18971	603.19153	3.0	427, 287, 269, 175, 147, 141, 139, 113
Met13	M24 (M14-Gluc)	U	$C_{28}H_{29}F_2N_4O_{10}$	619.18463	619.18534	1.1	443, 287, 269, 175, 147, 139, 113
Met14-1	—	F	$C_{22}H_{21}F_2N_4O_6S$	507.11444	507.11472	0.6	427, 303, 285, 191, 163, 139, 113
Met14-2	—	F	$C_{22}H_{19}F_2N_4O_5$	457.13180	457.13227	1.0	303, 285, 191, 179, 163, 139, 113
Met15-1	—	F	$C_{22}H_{21}F_2N_4O_4$	443.15254	443.15281	0.6	319, 301, 207, 179, 139, 125, 113
Met15-2	—	F	$C_{22}H_{21}F_2N_4O_4$	443.15254	443.15281	0.6	303, 285, 191, 179, 163, 139, 113
Met16-1	—	U	$C_{17}H_{18}FN_2O_4$	333.12451	333.12518	2.0	193, 141, 123
Met16-2	M13	P, U	$C_{22}H_{21}F_2N_4O_4$	443.15254	443.15324	1.6	425, 287, 269, 175, 147, 139, 113
Met17	M20 (M8-Gluc)	P, U	$C_{28}H_{29}F_2N_4O_9$	603.18971	603.18953	–0.3	479, 427, 303, 285, 283, 175, 155, 147, 129, 125
Met18	—	P	Unknown	—	—	—	—
Met19	—	F	$C_{22}H_{21}F_2N_4O_6S$	507.11444	507.11559	2.3	427, 287, 269, 175, 147, 139
Met20	M21 (M9-Gluc)	U	$C_{28}H_{29}F_2N_4O_9$	603.18971	603.19066	1.6	427, 287, 269, 175, 147, 139, 113
Met21-1	M11	P, U	$C_{17}H_{18}FN_2O_3$	317.12960	317.12927	–1.0	193, 125
Met21-2	M14	P, U	$C_{22}H_{21}F_2N_4O_4$	443.15254	443.15273	0.4	287, 269, 175, 157, 147, 139, 113
Met22-1	M1	F	$C_{22}H_{21}F_2N_4O_3$	427.15762	427.15805	1.0	303, 285, 191, 179, 163, 139, 125, 113
Met22-2	—	F	$C_{22}H_{21}F_2N_4O_4$	443.15254	443.15287	0.7	425, 319, 301, 207, 179, 139, 113
Met23	M15	P	$C_{22}H_{21}F_2N_4O_4$	443.15254	443.15278	0.5	287, 269, 175, 157, 147, 139, 113
Met24-1	M12	P, U, F	$C_{22}H_{19}F_2N_4O_4$	441.13689	441.13700	0.2	287, 269, 175, 147, 139, 113
Met24-2	M4	P, U	$C_{22}H_{21}F_2N_4O_3$	427.15762	427.15801	0.9	287, 269, 175, 147, 141, 139, 113

Met25	M7	F	$C_{22}H_{21}F_2N_4O_3$	427.15762	427.15817	1.3	303, 285, 191, 163, 139, 125, 113
Met26-1	M3	F	$C_{22}H_{21}F_2N_4O_3$	427.15762	427.15809	1.1	287, 269, 175, 147, 141, 139, 113
Met26-2	M9	P, F	$C_{22}H_{21}F_2N_4O_3$	427.15762	427.15785	0.5	287, 269, 175, 147, 141, 139, 113
Met27	M10	P	$C_{22}H_{21}F_2N_4O_3$	427.15762	427.15820	1.4	287, 269, 175, 147, 141, 139, 113
Met28	M8	F	$C_{22}H_{21}F_2N_4O_3$	427.15762	427.15791	0.7	303, 285, 283, 175, 155, 147, 129, 125
Met29	—	F	$C_{23}H_{21}F_2N_4O_4$	455.15254	455.15273	0.4	287, 269, 175, 169, 147, 139, 113

F: feces, Gluc: glucuronide, P: plasma, U: urine, —: not applicable.

Supplemental Figures

Supplemental Figure 1. Chemical structure of [^{14}C]lemborexant. Asterisk denotes the position of the ^{14}C label.

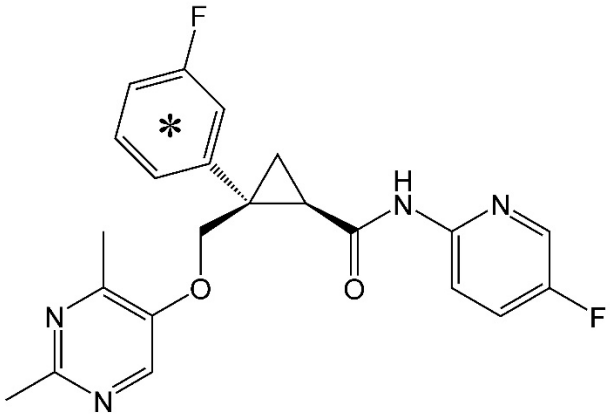

Supplemental Figure 2. Representative HPLC radiochromatograms of metabolites in human plasma, urine, and feces.